Analysis of lacrimal duct morphology from cone-beam computed tomography dacryocystography in a Japanese population

Jutaro Nakamura (jutaro_n@yokohama-cu.ac.jp)
Department of Ophthalmology and Visual Science, Yokohama City University Graduate School of Medicine

Tomoyuki Kamao
Department of Ophthalmology, Ehime University Graduate School of Medicine

Arisa Mitani
Department of Ophthalmology, Ehime University Graduate School of Medicine

Nobuhisa Mizuki
Department of Ophthalmology and Visual Science, Yokohama City University Graduate School of Medicine

Atsushi Shiraishi
Department of Ophthalmology, Ehime University Graduate School of Medicine

Research Article

Keywords: Dacryocystography, Cone-beam computed tomography, Dacryoendoscope, Primary acquired nasolacrimal duct obstruction, Endoscopic-assisted nasolacrimal duct intubation

Posted Date: April 11th, 2022

DOI: https://doi.org/10.21203/rs.3.rs-1137390/v4

Version of Record: A version of this preprint was published at Clinical Ophthalmology on June 23rd, 2022.
See the published version at https://doi.org/10.2147/OPTH.S370800.

Abstract

Purpose: The dacryoendoscope is a practical instrument for the examination and the treatment of lacrimal duct obstruction. Nevertheless, being a rigid fiberscope, manipulation of the endoscope is somewhat affected by the patient's lacrimal duct alignment and the skeletal structure of the face. The morphology and inclination of the lacrimal duct vary among individuals and ethnic groups. We aimed to evaluate the alignment of the lacrimal duct from the perspective of endoscopic maneuverability in a Japanese population.

Methods: This is the retrospective study analyzed the cone-beam computed tomography dacryocystography (CBCT-DCG) images of 102 patients diagnosed with unilateral primary acquired nasolacrimal duct obstruction (PANDO) at Ehime University Hospital from December 2015 to May 2021. The following parameters of the lacrimal duct on the contralateral side of unilateral PANDO were investigated: (1) angle formed by the superior orbital rim–internal common punctum–nasolacrimal duct opening, (2) angle formed by the lacrimal sac and the nasolacrimal duct, (3) length of the lacrimal sac, and (4) length of the nasolacrimal duct.

Results: Measurements of the above parameters were (1) 10.2° ± 7.8° (range, −11° to +27°), (2) −6.3° ± 14.1° (range, −43° to +40°), (3) 8.9 ± 2.3 mm (range, 4.3–17.1), and (4) 13.2 ± 2.7 mm (range, 5.7–20.7), respectively. The values of all parameters except (3) followed a normal distribution. No significant difference was found between the female and male groups.

Conclusions: This study reported anthropometric analysis data of the morphology of the lacrimal ducts using CBCT-DCG in a Japanese population. In our cohort, the line from the superior orbital rim through the internal common punctum to the nasolacrimal duct opening inclined anteriorly in 92% of the patients, which indicated that compared with using straight probes, utilizing a bent tip or a curved probe was considered more appropriate in reducing superior orbital rim interference.

Introduction

The lacrimal duct extends from the lacrimal punctum to the lower opening of the nasolacrimal duct (NLD) on the lateral wall of the inferior nasal meatus. It passes through the upper and lower puncta, the superior and inferior canaliculi, and the common canaliculus to reach the internal common punctum (ICP) on the tear sac. The pathway to this point passes through the eyelid tissue that is mobile and elastic. The lacrimal sac (LS) is fixed in the lacrimal fossa, and the interosseous and meatal parts of the NLD are also fixed tissues. Primary acquired nasolacrimal duct obstruction (PANDO) is an organic obstruction of the lacrimal duct that can occur anywhere from the punctum to NLD opening on the inferior nasal meatus.[1] Cases with obstruction from the punctum to the ICP are classified as *pre-saccal obstruction*, whereas cases with obstruction thereafter are classified as *post-saccal obstruction*.

Since it was first reported in 1909, dacryocystography (DCG) has undergone improvements in contrast media, injection methods, and image capturing methods. DCG is still an essential preoperative evaluation

for PANDO.[2,3] Meanwhile, clinical applications of cone-beam computed tomography (CBCT) have gradually increased in the head and neck regions since its first application in dentistry in 1998. CBCT is now widely used in medical facilities for dentistry, oral surgery, and otorhinolaryngology.[4-7] Despite the limited reports on CBCT usage in ophthalmology, CBCT-DCG remains a practical test for evaluating PANDO. It has the advantage of considerably lower radiation exposure than conventional multi-slice CT-DCG.[8-10]

Dacryocystorhinostomy (DCR) is the first-line treatment for PANDO. Meanwhile, endoscopic-assisted nasolacrimal duct intubation (ENDI) is widely utilized as a minimally invasive treatment for lacrimal duct stenosis and obstruction in Northeast Asia.[11-14] The ENDI procedure is performed while directly observing the obstructed region in the lacrimal duct with a dacryoendoscopy and observing the inferior meatus in the nasal cavity with a nasal endoscopy (Supplementary file, Video 1). This procedure reduces complications from the formation of an iatrogenic false passage. Since ENDI can be usually performed under local anesthesia, it has evolved into a less invasive and more secure procedure, which is one of the main reasons for its increasingly widespread use in Northeast Asia. Moreover, Northeast Asians have relatively flat facial features, with a less elevated superior orbital rim (SOR) than other ethnic groups. This allows for relatively easy manipulation of a dacryoendoscope.[15]

The line formed by the SOR–ICP is the anatomical limit where the tip of a straight probe can reach most anteriorly after entering the NLD through the ICP. When the line formed by the ICP–NLD opening was anteriorly inclined to the line formed by the SOR–ICP, blind probing with a straight bougie or manipulating a dacryoendoscope with a straight probe might create an iatrogenic false passage posterior to the original lacrimal duct. Because it allows the endoscope to stand more vertically than the SOR; however, it is more difficult to tilt it horizontally than the SOR (Figs. 1, 2).

The maneuverability of the endoscope in the lacrimal sac and the nasolacrimal duct is often interfered with by the elevated superior orbital rim. The higher the superior orbital rim, the more difficult it is to manipulate the endoscope; the lower, the more manageable it is to handle. This study aimed to investigate the morphology and anthropometric features of the lacrimal duct from the perspective of endoscopic maneuverability. The length, morphology, and inclination of the lacrimal duct was reported to be different among individuals, and differences were also reported between races and ethnic groups. [16-21] Hence, this study investigated the angle of the SOR–ICP–NLD opening, LS–NLD inclination, and the lengths of the LS and NLD to evaluate the anthropometric features of the lacrimal duct morphology in a Japanese population.

Materials And Methods

Patient selection

The study included patients diagnosed with unilateral PANDO at Ehime University Hospital from December 2015 to April 2021. The diagnosis was obtained through irrigation test, dacryoendoscopic

examination, and CBCT-DCG. We retrospectively analyzed the CBCT-DCG images of the contralateral side of 102 patients diagnosed with unilateral PANDO. No abnormalities were found on the contralateral side in any of the above tests. A typical example of a CBCT-DCG image sectioning the lacrimal duct is shown in Fig. 3. The patient had been diagnosed with left-sided unilateral PANDO. Fig. 3 shows a DCG image of the right side, contralateral to the obstructed side.

DCG and CBCT procedures

After topical anesthesia with 4% lidocaine instillation, a 23-gauge curved lacrimal cannula was inserted into the upper and lower puncta. A nonionic, water-soluble contrast agent (1–2 mL; Omnipaque 300® [iohexol]; GE Healthcare, Tokyo, Japan) was manually injected slowly until the patient reported that the solution reached the nasal antrum or until the contrast agent flowed back from the punctum. CBCT was performed within 10 min after injection of the contrast medium. CBCT images were acquired using a 3D Accuitomo F17 (Morita, Kyoto, Japan). The imaging conditions were a scan time of 17.5 s and X-ray output of 90 kV and 8.0 mA. The length and angle measurements from the images were made using dedicated computer software (i-Dixel 2.0; Morita, Kyoto, Japan). The images were converted to monochrome to facilitate observation of the contrast media.

Investigated parameters on CBCT-DCG images

Four parameters were evaluated in CBCT-DCG images of a sagittal section: (1) Angle formed by SOR–ICP–NLD opening (Fig. 4A). The described method was applied to evaluate this angle. A straight line starting from the ICP was drawn in the direction of the SOR and the tangent point on the SOR was determined. The distal end of the interosseous NLD was defined as the NLD opening. Then, the angle formed by the line connecting the tangent point of SOR–ICP and the line connecting ICP–NLD opening was measured.

Other parameters measured include (2) the angle formed by LS–NLD (Fig. 4B), (3) length from the ICP to the LS–NLD transition (LS length) (Fig. 4C), and (4) length from the LS–NLD transition to the NLD opening (NLD length) (Fig. 4C). Of the above, parameter (2) refers to the angle formed by the long axis of the LS and the nasolacrimal duct at the LS–NLD transition. The angles were designated by positive and negative values in the anterior and posterior bending types, respectively. The LS–NLD transition was determined by the sagittal projection of the area corresponding to the origin of the interosseous NLD in the horizontal section of the CBCT image.

Statistical analysis

Data were analyzed using JMP software ver. 16 (SAS Institute, Cary, NC, USA). The Shapiro–Wilk test was used to determine whether measurement data followed a normal distribution; a *p*-value of >0.05 was considered to indicate normality in the distribution. The Mann–Whitney U test was used to test the significance of differences for each parameter between the male and female groups. A *p*-value of <0.05 was considered significant.

Ethical approval and consent to participate

This study and its data collection protocol were approved by the Institutional Review Board of Ehime University (Ethical approval no. 1601003). The study was registered with the University Hospital Medical Information Network Clinical Trials Registry (No. UMIN 000025180). Written informed consent was obtained from each patient before enrollment. All procedures used in this study were performed in accordance with the tenets of the Declaration of Helsinki.

Results

The mean age of the 102 patients was 71.3 ± 11.7 years. Among them, 74 patients were female and 28 were male. There were 51 cases of right-side PANDO and 51 cases of left-side PANDO. The maximum, minimum, and average values of the measured parameters are shown in Table 1.

Angle formed by the SOR–ICP–NLD opening

The maximum and the minimum values of the angle were 27° and −11°, respectively, and the mean value was 10.2° ± 7.8°. The angle was positive in 92% (93/101) of cases, whereas it was negative in 8% (8/101) of the patients. An example image of a case with a large SOR–ICP–NLD opening angle is shown in Fig. 5. The large angle was caused by the elevation of the SOR and anterior inclination of the NLD. The Shapiro–Wilk test gave a value of 0.55, indicating a normal distribution (Fig. 6A). For the female group, the mean was 9.9° ± 8.2°; for the male group, it was 10.8° ± 6.7°. No significant difference was found between the male and female groups ($p = 0.67$).

LS–NLD angle

The maximum and minimum angles were 40° and −43°, respectively, and the mean angle was −6.3° ± 14.1°. The Shapiro–Wilk test gave a value of 0.30, indicating a normal distribution (Fig. 6B). The anterior and posterior bending types represented 33.3% (31/93) and 66.7% (62/93) of the cases, respectively. Examples of cases with anterior and posterior bending types are shown in Figs. 7 and 8, respectively. The mean LS–NLD angles for the female and male groups were −6.9° ± 14.5°, and −4.6° ± 12.9°, respectively. No significant difference was found between the male and female groups ($p = 0.29$).

LS length

The maximum and minimum LS lengths were 17.1 mm and 4.3 mm, respectively, and the mean was 8.9 ± 2.3 mm. The Shapiro–Wilk test gave a value of 0.0002, indicating a non-normal distribution (Fig. 6C). The mean LS lengths for the female and male groups were 8.7 ± 2.1 mm and 9.6 ± 2.6 mm, respectively. No significant difference was found between the female and male groups (p = 0.079).

NLD length

The maximum and minimum values were 20.7 mm and 5.7 mm, respectively, and the mean value was 13.2 ± 2.7 mm. The Shapiro–Wilk test gave a value of 0.39, showing a normal distribution (Fig. 6D). The mean NLD length for the female and male groups were 13.0 ± 2.4 mm and 13.7 ± 3.3 mm, respectively. No significant difference was found between the female and male groups (p = 0.17).

Discussion

DCR is the first-line treatment for PANDO in Western countries. Meanwhile, ENDI is employed as a minimally invasive treatment in Northeast Asia (Supplementary file, Video 1). Generally, the long-term therapeutic outcomes of ENDI are not equivalent to those of DCR. Nevertheless, accumulating evidence has revealed that the outcomes of ENDI are almost as effectual as those of DCR for canaliculus obstruction and certain forms of PANDO (in cases of non-inflammatory or partial obstruction).[11,13,14,22-24] Since ENDI can be a minimally invasive procedure for the treatment of PANDO, further studies are needed to compare the long-term treatment outcomes of DCR and ENDI in terms of pathological conditions (e.g., site of obstruction, cause of obstruction, and duration of obstruction).

The lengths and morphologies of the lacrimal duct vary among individuals and ethnic groups.[16-21] In this study, we examined several parameters of the lacrimal duct using sagittal CBCT-DCG images in a Japanese population. Results showed the average angle formed by the SOR–ICP–NLD opening was 10.2° ± 7.8°. As mentioned above, the line formed by the SOR–ICP is the anatomical limit where the tip of a straight probe can reach most anteriorly after entering the NLD through the ICP. We confirmed that in 92% of the patients in our cohort, the line formed by the ICP–NLD opening was anteriorly inclined to the SOR–ICP line. This suggests that blind probing with straight bougies or manipulating a dacryoendoscope with straight probes pose risks for forming an iatrogenic false passage posterior to the original lacrimal duct in this cohort. Therefore, a probe with a bent anterior tip, or a curved probe, would be more appropriate in these cases (Fig. 9). In 8% of the patients, the SOR–ICP–NLD angle was zero or negative. In such cases, a straight probe is considered more suitable than a probe with a bent anterior tip or with a curved tip.

Generally, Northeast Asians have a low rate of development of the SOR and portray a relatively flat facial appearance. The SOR–ICP–NLD angle in other ethnic groups that have a well-developed SOR may be different from our study's results. Examining several other races and ethnic groups will reveal the diversity of the SOR–ICP–NLD angles in different ethnic groups.

We also investigated the LS–NLD angle and found a mean value of −6.3° ± 14.1° (range, −43° to +40°). The average angles of the anterior and posterior bending types (33.3% of cases, Fig. 7) were 8.8° ± 14.1° and (66.7% of cases, Fig. 8) −13.8°± 13.3°, respectively. Previous studies have reported the LS–NLD angle in an anatomical survey of Japanese cadavers; Narioka et al. reported that the anterior bending type accounted for 80% of cases, with an average angle of +8.9 ± 5.0° (range, 0°–19°), and the posteriorly bending type accounted for 20% of cases, with an average angle of −12.3 ± 9.0° (range, −2° to −26°).[25] By contrast, Park et al. reported that the mean LS–NLD angle was −10.3° and that approximately 90% of cases had posterior bending.[26] In this study, our data were provided by a relatively larger number of cases than the previous reports; however, it is still necessary to increase the number of measurements and accumulate data on the LS–NLD angle and the frequencies of anterior and posterior bending variations for attaining more accurate values.

There are several limitations to this study. First, we did not evaluate normal lacrimal duct morphology; we evaluated the contralateral lacrimal duct of patients diagnosed with unilateral PANDO. We cannot exclude the possibility that a unilateral PANDO case in this study might develop into a bilateral PANDO. Second, our measurements were obtained from two-dimensional images; in essence, we need to obtain measurements in three dimensions. It has been reported that in coronal sections, the LS is inclined laterally to the midline and the NLD is inclined medially to the LS. Moreover, approximately one-third of the NLDs are medially inclined, and two-thirds are laterally inclined, relative to the midline.[25] Furthermore, the NLD does have a linear structure but bends in complicated and diverse ways. Although we used planimetric data in sagittal sections, the actual lengths and constituent angles of a lacrimal duct should be represented in three dimensions.

Conclusion

One of the serious complications of ENDI surgery is forming a false passage. The creation of false passage results not only from the firmness of the obstruction site but also from the fact that the lacrimal duct often runs beyond the range of motion of the endoscope probe. The maneuverability of the endoscope in the LS and NLD is often interfered with by the elevated SOR. This study investigated anthropometric data analyzing the morphology of the lacrimal ducts using CBCT-DCG in a Japanese population. In over 90% of the patients in our cohort, the SOR–ICP–NLD angle was inclined anteriorly, indicating that employing a dacryoendoscope probe with a bent tip or curved probe was considered reasonable in reducing SOR interference in these cases.

Declarations

Acknowledgments

This study was supported by the Japan Society for the Promotion of Science (JSPS) Postdoctoral Fellowship for Research Abroad (Kaitoku-NIH, #24112 to JN). The funding source had no role in the study design, data collection, and analysis, decision to publish, or preparation of the manuscript.

Conflict of interest

The authors declare that they have no competing interests. The authors alone are responsible for the content and writing of the paper.

Author Contributions

JN contributed to conception, data extraction, analysis, and drafting. TK performed the surgical procedure, data extraction, interpretation of the results and drafting. AM and AS performed the surgical procedures, data acquisition, and interpretation of the results. TK, AM, and AS provided statistical advice. NM and AS provided general management of the study. NM and AS critically revised the protocol and main manuscript.

Data availability

The datasets analyzed in this study are available from the corresponding author (JN) on reasonable request.

Bibliography

1. Mandeville JT, Woog JJ. Obstruction of the lacrimal drainage system. *Curr Opin Ophthalmol*. Oct 2002;13(5):303-9. doi:10.1097/00055735-200210000-00003

2. Montecalvo RM, Zegel HG, Barnett FJ, et al. Evaluation of the lacrimal apparatus with digital subtraction macrodacryocystography. *Radiographics*. May 1990;10(3):483-90. doi:10.1148/radiographics.10.3.2188309

3. Singh S, Ali MJ, Paulsen F. Dacryocystography: From theory to current practice. *Annals of Anatomy - Anatomischer Anzeiger*. 2019/07/01/ 2019;224:33-40. doi:https://doi.org/10.1016/j.aanat.2019.03.009

4. Cakli H, Cingi C, Ay Y, Oghan F, Ozer T, Kaya E. Use of cone beam computed tomography in otolaryngologic treatments. *Eur Arch Otorhinolaryngol*. Mar 2012;269(3):711-20. doi:10.1007/s00405-011-1781-x

5. Mozzo P, Procacci C, Tacconi A, Martini PT, Andreis IA. A new volumetric CT machine for dental imaging based on the cone-beam technique: preliminary results. *Eur Radiol*. 1998;8(9):1558-64. doi:10.1007/s003300050586

6. Nasseh I, Al-Rawi W. Cone Beam Computed Tomography. *Dent Clin North Am*. Jul 2018;62(3):361-391. doi:10.1016/j.cden.2018.03.002

7. Patel S, Brown J, Pimentel T, Kelly RD, Abella F, Durack C. Cone beam computed tomography in Endodontics - a review of the literature. *Int Endod J*. Aug 2019;52(8):1138-1152. doi:10.1111/iej.13115

8. Suzuki T. CT and CT-Dacryocystography for Patient Selection in Nasolacrimal Duct Intubation. *Journal of the Eye*. 2015/12 2015;32(12):1673-1680.

9. Tschopp M, Bornstein MM, Sendi P, Jacobs R, Goldblum D. Dacryocystography using cone beam CT in patients with lacrimal drainage system obstruction. *Ophthalmic Plast Reconstr Surg*. Nov-Dec 2014;30(6):486-91. doi:10.1097/iop.0000000000000154

10. Wilhelm KE, Rudorf H, Greschus S, et al. Cone-Beam Computed Tomography (CBCT) dacryocystography for imaging of the nasolacrimal duct system. *Klin Neuroradiol*. Dec 2009;19(4):283-91. doi:10.1007/s00062-009-9025-9

11. Javate RM, Pamintuan FG, Cruz RT, Jr. Efficacy of endoscopic lacrimal duct recanalization using microendoscope. *Ophthalmic Plast Reconstr Surg*. Sep-Oct 2010;26(5):330-3. doi:10.1097/IOP.0b013e3181c7577a

12. Kamao T, Takahashi N, Zheng X, Shiraishi A. Changes of Visual Symptoms and Functions in Patients with and without Dry Eye after Lacrimal Passage Obstruction Treatment. *Curr Eye Res*. May 3 2020:1-8. doi:10.1080/02713683.2020.1760305

13. Kamao T, Zheng X, Shiraishi A. Outcomes of bicanalicular nasal stent inserted by sheath-guided dacryoendoscope in patients with lacrimal passage obstruction: a retrospective observational study. *BMC Ophthalmol*. Feb 25 2021;21(1):103. doi:10.1186/s12886-020-01678-5

14. Lee SM, Lew H. Transcanalicular endoscopic dacryoplasty in patients with primary acquired nasolacrimal duct obstruction. *Graefes Arch Clin Exp Ophthalmol*. Jan 2021;259(1):173-180. doi:10.1007/s00417-020-04833-2

15. Whitnall SE. Anatomy of the Human Orbit and Accessory Organs of Vision. *Krieger Publishing, Huntington, NY*. 1979;

16. Maliborski A, Różycki R. Diagnostic imaging of the nasolacrimal drainage system. Part I. Radiological anatomy of lacrimal pathways. Physiology of tear secretion and tear outflow. *Med Sci Monit*. 2014;20:628-638. doi:10.12659/MSM.890098

17. Paulsen F. [Anatomy and physiology of efferent tear ducts]. *Ophthalmologe*. Apr 2008;105(4):339-45. Anatomie und Physiologie der ableitenden Tränenwege. doi:10.1007/s00347-008-1735-x

18. Valencia MRP, Takahashi Y, Naito M, Nakano T, Ikeda H, Kakizaki H. Lacrimal drainage anatomy in the Japanese population. *Ann Anat*. May 2019;223:90-99. doi:10.1016/j.aanat.2019.01.013

19. Kim YH, Park MG, Kim GC, Park BS, Kwak HH. Topography of the nasolacrimal duct on the lateral nasal wall in Koreans. *Surg Radiol Anat*. Apr 2012;34(3):249-55. doi:10.1007/s00276-011-0858-y

20. Sahni S, Goyal R, Gupta T, Gupta A. Surgical Anatomy of Nasolacrimal Duct and Sac in Human Cadavers. *Clinical Rhinology An International Journal*. 12/01 2014;7:91-95. doi:10.5005/jp-journals-10013-1205

21. Ali MJ, Schicht M, Paulsen F. Morphology and morphometry of lacrimal drainage system in relation to bony landmarks in Caucasian adults: a cadaveric study. *Int Ophthalmol*. Dec 2018;38(6):2463-2469. doi:10.1007/s10792-017-0753-6

22. Matsumura N, Suzuki T, Goto S, et al. Transcanalicular endoscopic primary dacryoplasty for congenital nasolacrimal duct obstruction. *Eye (Lond)*. Jun 2019;33(6):1008-1013. doi:10.1038/s41433-019-0374-6

23. Mimura M, Ueki M, Oku H, Sato B, Ikeda T. Indications for and effects of Nunchaku-style silicone tube intubation for primary acquired lacrimal drainage obstruction. *Jpn J Ophthalmol*. Jul 2015;59(4):266-72. doi:10.1007/s10384-015-0381-5

24. Sugimoto M, Inoue Y. Long-term Outcome of Dacryoendoscope-assisted Intubation for Nasolacrimal Duct Obstruction. *Journal of the eye*. 2010;27(9):1291-1294.

25. Narioka J, Matsuda S, Ohashi Y. Correlation between anthropometric facial features and characteristics of nasolacrimal drainage system in connection to false passage. https://doi.org/10.1111/j.1442-9071.2007.01558.x. *Clinical & Experimental Ophthalmology*. 2007/09/01 2007;35(7):651-656. doi:https://doi.org/10.1111/j.1442-9071.2007.01558.x

26. Park J, Takahashi Y, Nakano T, et al. The orientation of the lacrimal fossa to the bony nasolacrimal canal: an anatomical study. *Ophthalmic Plast Reconstr Surg*. Nov-Dec 2012;28(6):463-6. doi:10.1097/IOP.0b013e31826463d9

Tables

Table 1. Lacrimal duct parameters measured on sagittal sections of CBCT-DCG images

	1	2	3	4
Parameters	**SOR–ICP–NLD opening angle**	**LS–NLD angle**	**LS length**	**NLD length**
Description	Angle formed by the superior orbital rim, internal common punctum, and nasolacrimal duct opening	Angle formed by the lacrimal sac and the nasolacrimal duct	Length from the internal common punctum to the transition	Length from the transition to the nasolacrimal duct opening
Mean value	10.2° ± 7.8°	−6.3° ± 14.1°	8.9 ± 2.3 mm	13.2 ± 2.7 mm
Maximum value	27°	40°	17.1 mm	20.7 mm
Minimum value	−11°	−43°	4.3 mm	5.7 mm
***p*-value[*1]**	0.5528	0.3007	0.0002	0.3946
Normal distribution	Yes	Yes	No	Yes
Mean values of the female group	9.9° ± 8.2°	−6.9° ± 14.5°	8.7 ± 2.1 mm	13.0 ± 2.4 mm
Mean values of the male group	10.8° ± 6.7°	−4.6° ± 12.9°	9.6 ± 2.6 mm	13.7 ± 3.3 mm
***p*-value[*2]**	0.6706	0.2862	0.0785	0.1723
Sexual difference	None	None	None	None

Note: *[1] The *p*-value in the normal distribution column was calculated by the Shapiro–Wilk test; $p > 0.05$ indicated that the distribution was normal. *[2] The non-parametric Mann–Whitney U test was used to compare the male and female groups. The results were considered significant at a *p*-value of < 0.05.

Abbreviations: CBCT-DCG, cone-beam computed tomography dacryocystography; ICP, internal common punctum; LS, lacrimal sac; NLD, nasolacrimal duct; SOR, superior orbital rim.

Figures

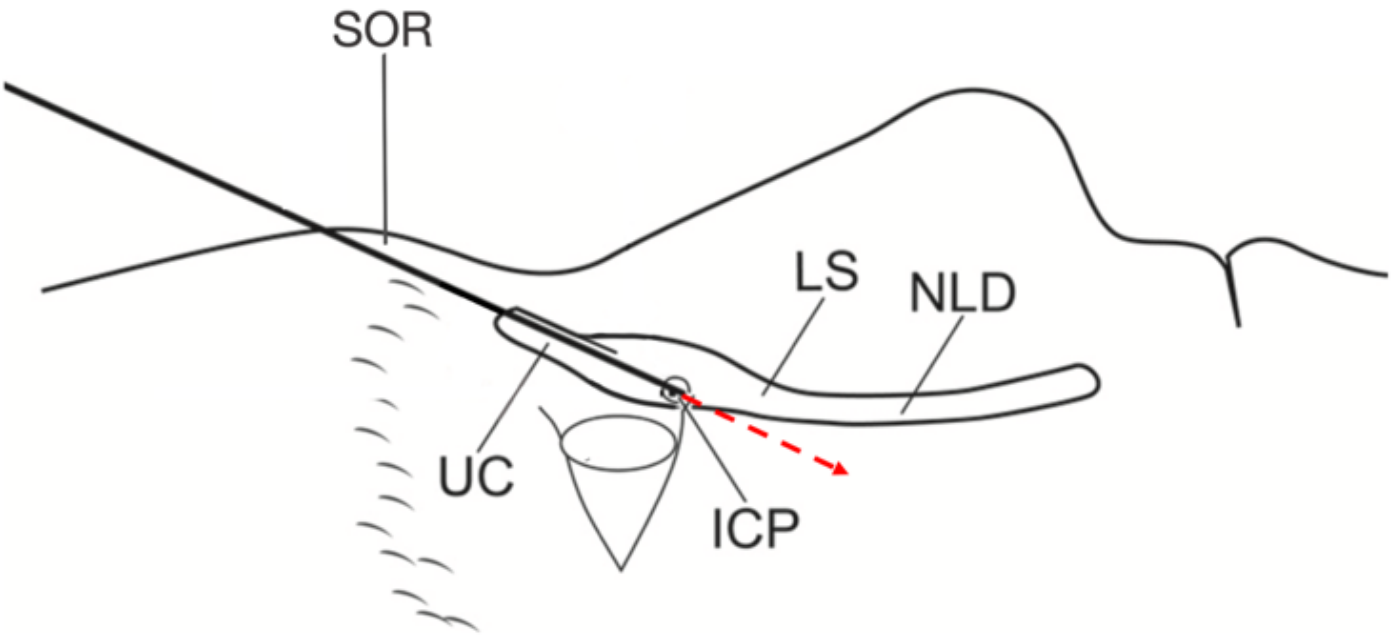

Figure 1

SOR–ICP line as an anatomical limitation

The line formed by the SOR–ICP is the anatomical limit where the tip of a straight probe can reach most anteriorly after entering the LS through the ICP. The red arrow indicates when the LS and NLD inclined anteriorly to the line formed by the SOR–ICP. Manipulating straight probes poses a risk for forming an iatrogenic false passage posterior to the original lacrimal duct.

Abbreviations: ICP, internal common punctum; LS, lacrimal sac; NLD, nasolacrimal duct; SOR, superior orbital rim; UC, upper canaliculus

Figure 2

SOR interference during manipulation of the dacryoendoscope

SOR interferes the manipulation of the endoscope. It is difficult to tilt the probe horizontally than the SOR. However, the endoscope can stand more vertically than the SOR.

Abbreviation: SOR, superior orbital rim

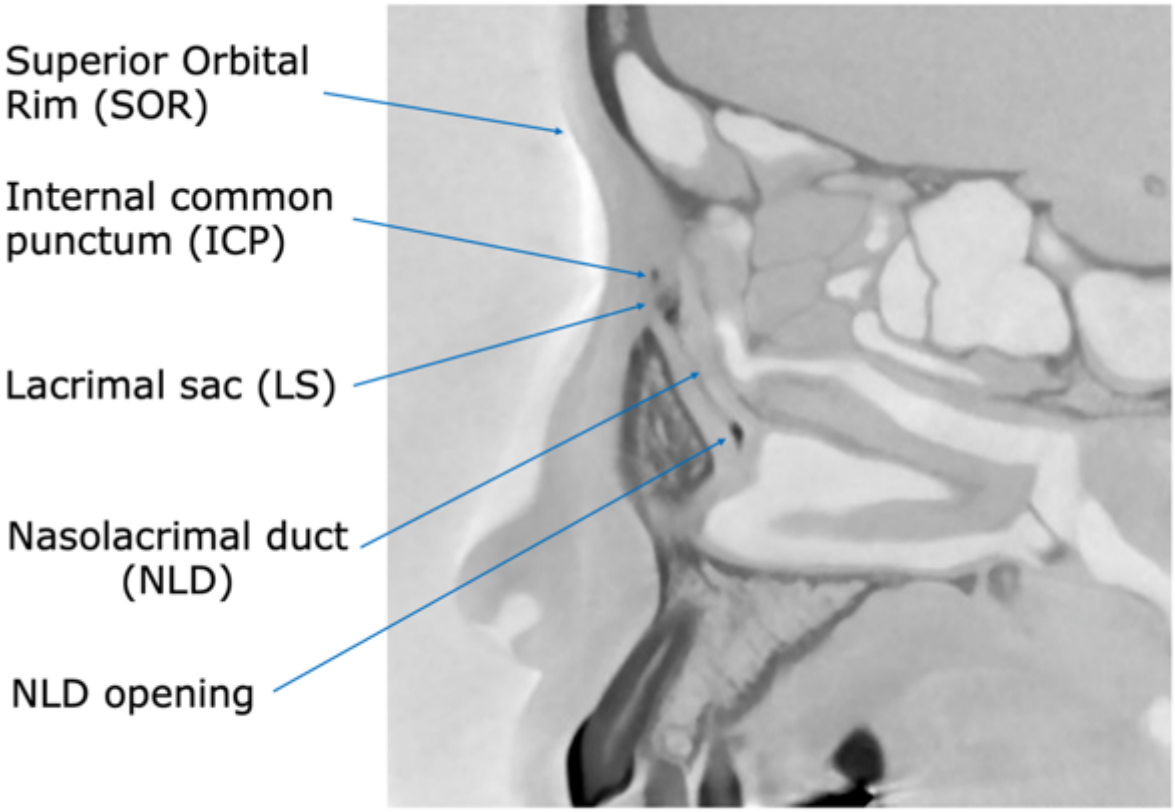

Figure 3

CBCT-DCG sagittal image sectioning the lacrimal duct

The figure shows a dacryocystographic image of the nasolacrimal duct on the right side from a patient diagnosed with left-sided unilateral primary acquired nasolacrimal duct obstruction. The original image was converted to monochrome to facilitate observation of the contrast media.

Abbreviations: CBCT-DCG, cone-beam computed tomography–dacryocystography.

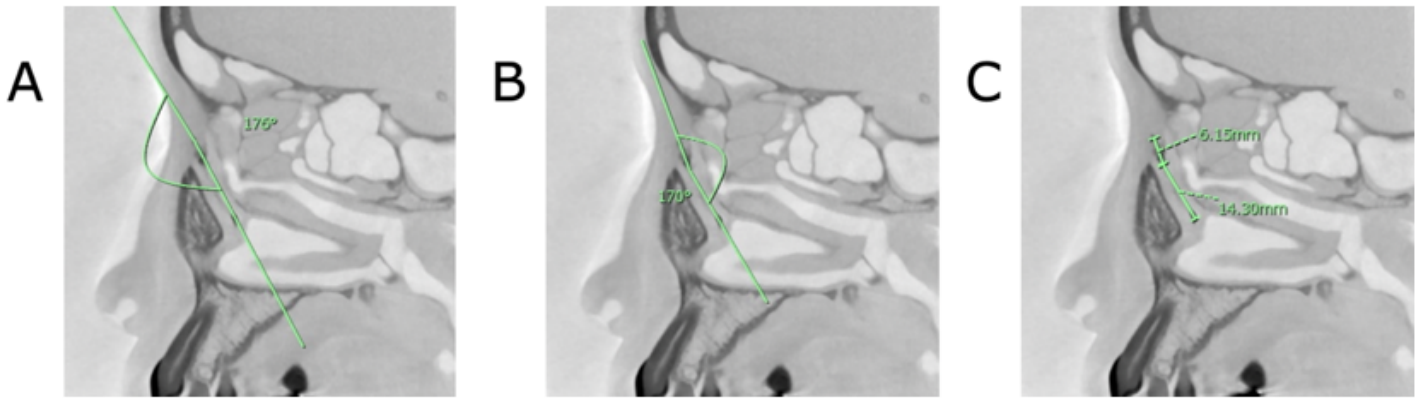

Figure 4

Parameters measured in CBCT-DCG images

(A) Angle formed by SOR–ICP–NLD opening. In this case, the line connecting the ICP–NLD opening was inclined anteriorly at 4° relative to the line connecting the SOR–ICP. (B) Angle formed by LS and NLD. In this case, the long axis of the NLD was inclined posteriorly at 10° relative to the LS. (C) Length of LS and NLD, with 6.15 mm and 14.30 mm, respectively.

Abbreviations: CBCT-DCG, cone-beam computed tomography–dacryocystography; SOR, superior orbital rim; ICP, internal common punctum; LS, lacrimal sac; NLD, nasolacrimal duct.

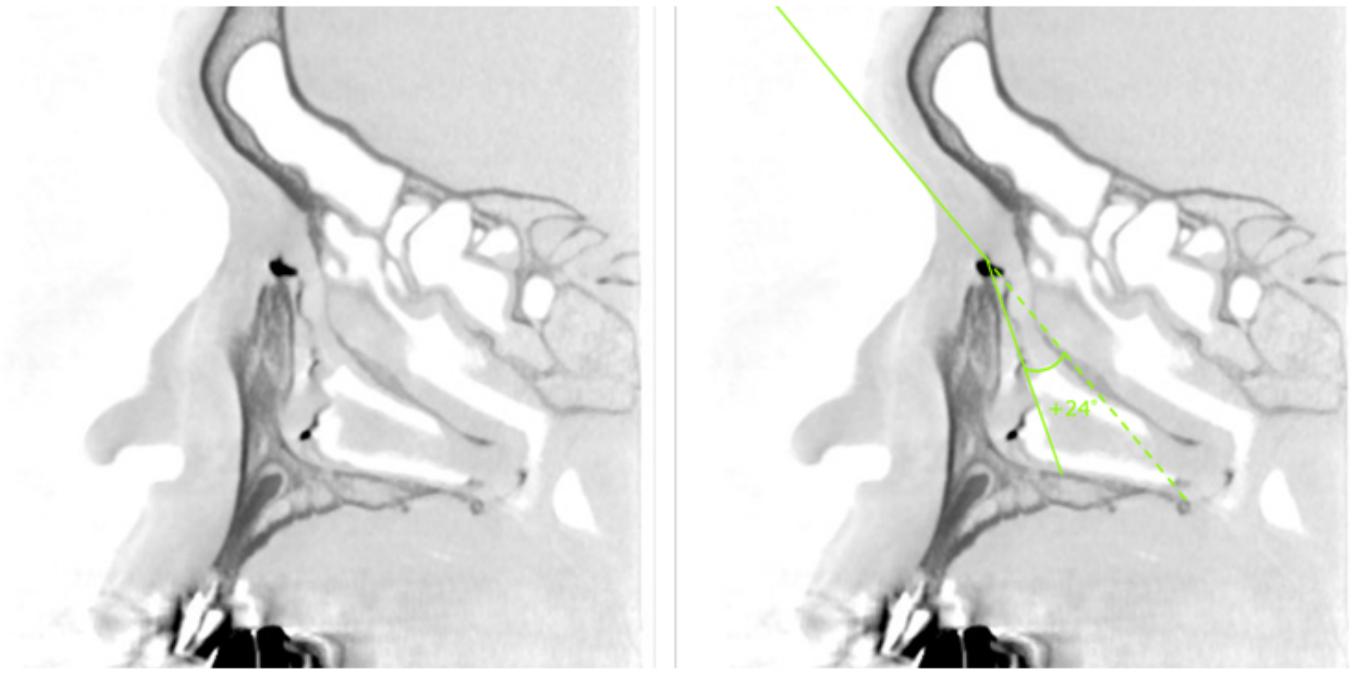

Figure 5

Example of a large SOR–ICP–NLD opening angle

On the left side is the original image. On the right side, a relatively large angle of 24° is seen, which is due to the elevation of the SOR and the anterior inclination of the NLD.

Abbreviations: ICP, internal common punctum; NLD, nasolacrimal duct; SOR, superior orbital rim.

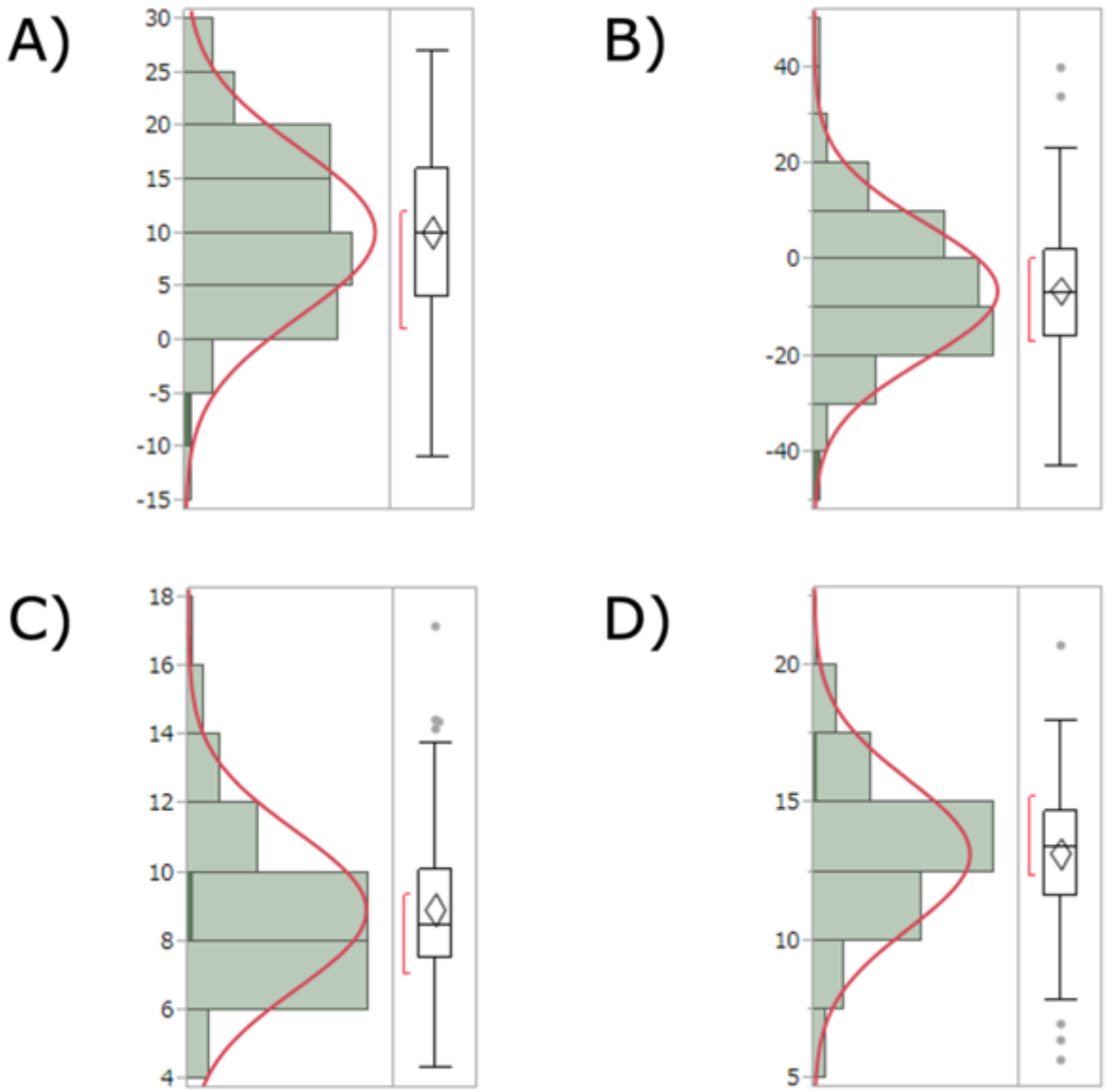

Figure 6

Test results for the normal distribution of the measured parameters

(A) *SOR–ICP–NLD opening angle*: The average angle was 10.7° ± 7.4° (range, −6° to +27°) and followed a normal distribution (p = 0.55). **(B)** *LS–NLD angle*: The mean angle was −6.84° ± 13.7° (range, −43° to +34°) and followed a normal distribution (p = 0.28). **(C)** *LS length*: The mean length was 8.9 ± 2.2 mm (range, 5.4–17.1) and did not follow a normal distribution (p = 0.078). **(D)** *NLD length*: The mean length was 13.3 ± 2.7 mm (range, 5.7–20.7) and followed a normal distribution (p = 0.17). The p-value was determined by the Shapiro–Wilk test. A p-value of >0.05 indicated a normal distribution.

Abbreviations: ICP, interior common punctum; LS, lacrimal sac; NLD, nasolacrimal duct; SOR, superior orbital rim.

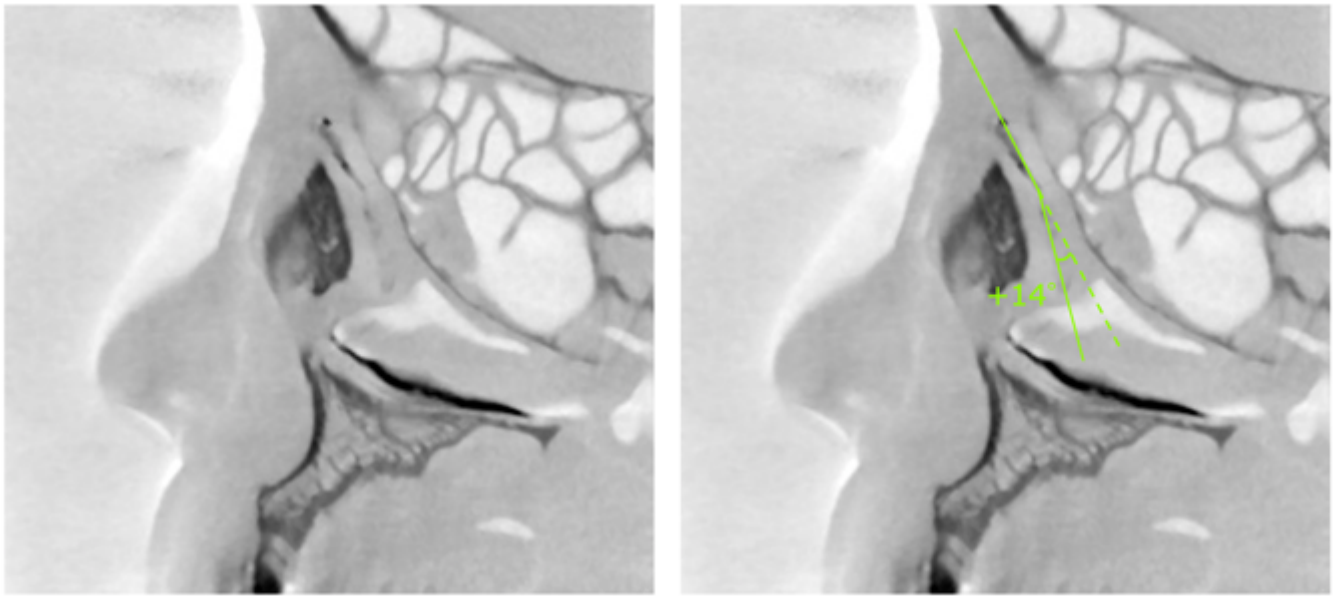

Figure 7

Case in which the NLD is inclined anteriorly to the LS (anterior bending type)

On the left is the original image. On the right side, the long axis of the NLD was anteriorly inclined by +14° relative to that of the LS.

Abbreviations: LS, lacrimal sac; NLD, nasolacrimal duct.

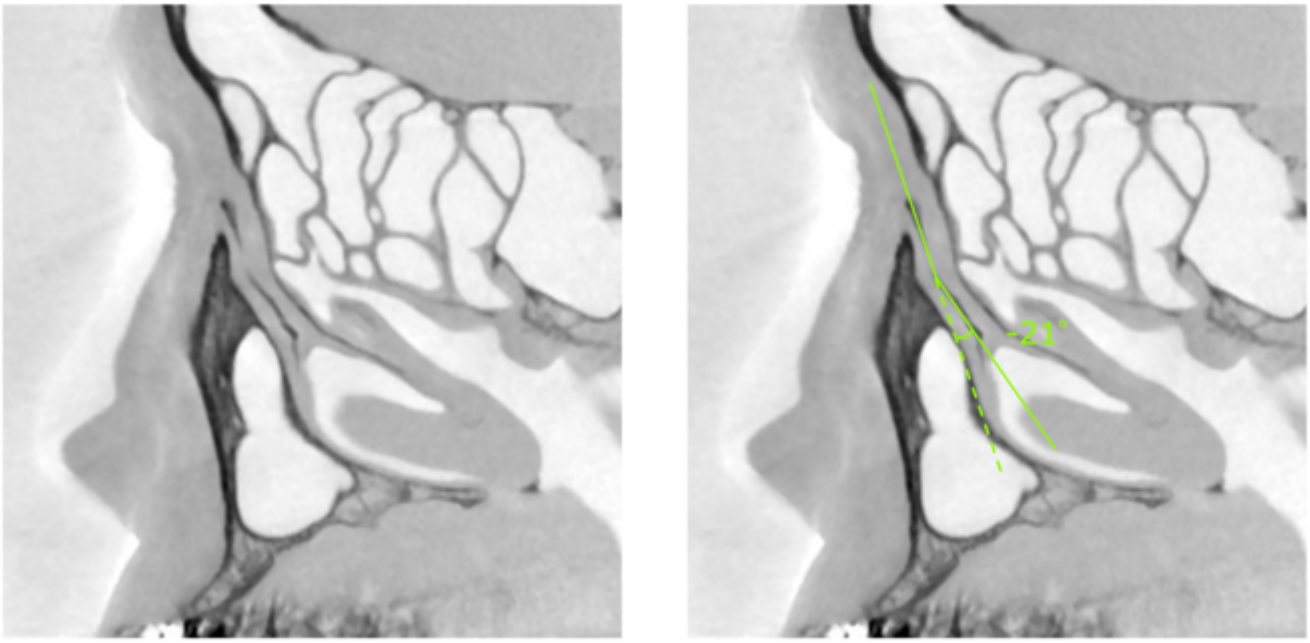

Figure 8

Case in which the NLD is inclined posteriorly to the LS (posterior bending type)

On the left is the original image. On the right side, the long axis of the NLD was posteriorly inclined by −21° relative to the LS.

Abbreviations: LS, lacrimal sac; NLD, nasolacrimal duct.

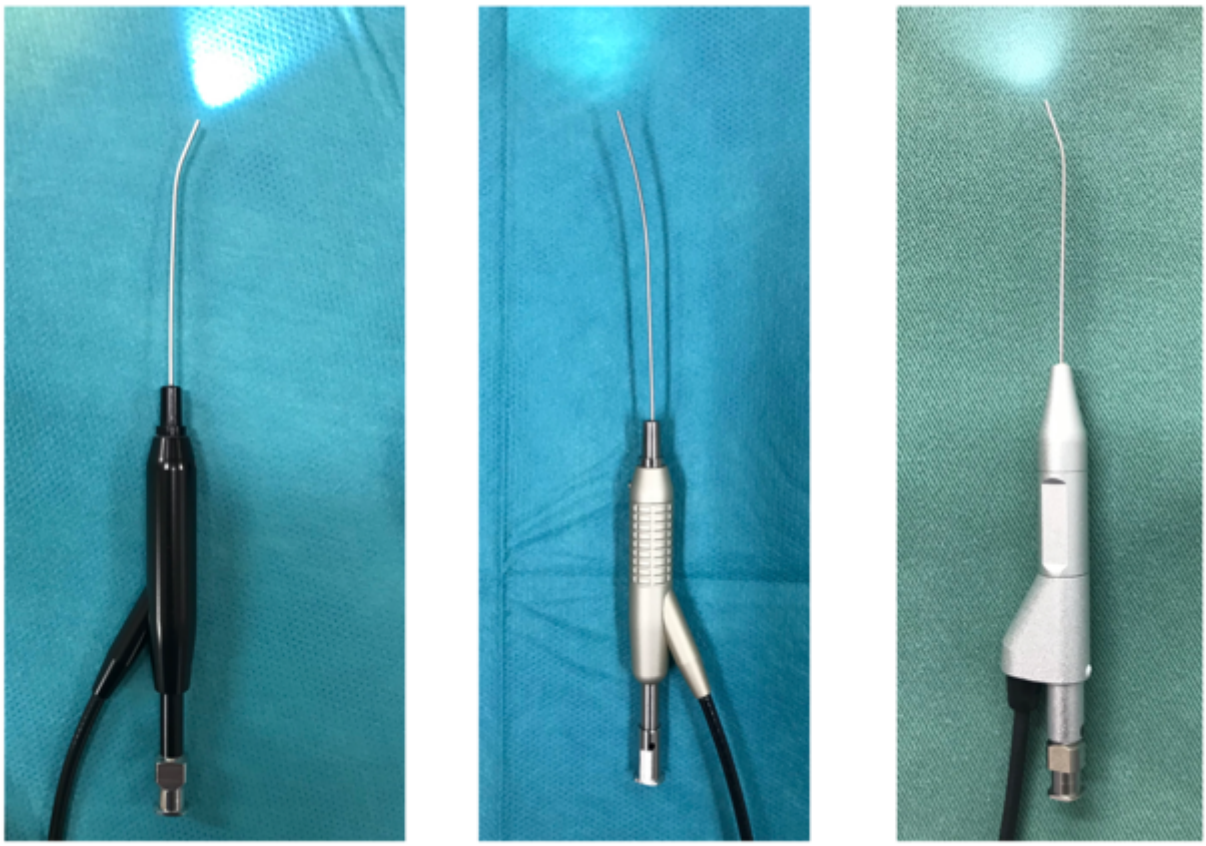

Figure 9

Dacryoendoscope with an anteriorly bent tip probe and a curve-tipped probe

Left: CK10® (FiberTech Co., Ltd., Tokyo, Japan); external diameter, 0.9mm; field of view, 60°; image quality, 10,000 pixels

Middle: CH15C® (FiberTech Co., Ltd., Tokyo, Japan); external diameter, 0.82 mm; field of view, 70°; image quality, 15,000 pixels

Right: LAC-06-FY® (Machida Endoscope Co., Ltd., Chiba, Japan); external diameter, 0.9 mm; field of view, 65°; image quality, 15,000 pixels

Supplementary Files

This is a list of supplementary files associated with this preprint. Click to download.

- Video1.mp4